Hindawi
Advances in Civil Engineering
Volume 2021, Article ID 6644471, 14 pages
https://doi.org/10.1155/2021/6644471

Research Article

Pore-Size Distribution Evolution of Intact, Compacted, and Saturated Loess from China during Consolidation and Shearing

Ping Li,[1,2,3] **Shengjun Shao**,[2] **Tao Xiao**,[1] **and Dandan Zhu**[2]

[1]*State Key Laboratory of Continental Dynamics, Department of Geology, Northwest University, Xi'an 710069, China*
[2]*Shaanxi Key Laboratory of Loess Mechanics and Engineering, Civil Engineering and Architecture Institute, Xi'an University of Technology, Xi'an 710048, China*
[3]*Water Cycle and Geological Environment Observation and Research Station for the Chinese Loess Plateau, Ministry of Education, Zhengning 745399, Gansu, China*

Correspondence should be addressed to Ping Li; lp19881028@163.com and Shengjun Shao; sjshao@xaut.edu.cn

Received 8 December 2020; Revised 15 January 2021; Accepted 5 February 2021; Published 19 February 2021

Academic Editor: Jian Xu

To examine the pore-size distribution (PSD) evolution of intact, compacted, and saturated loess during deformation associated with consolidation or shearing, nominally identical specimens were consolidated to different confining stresses or sheared to sequential axial strains under the same confining stress, and the PSD of each deformed specimen was characterized using the Mercury intrusion porosimetry (MIP) technique. The results show that the PSD evolution during consolidation is similar to that during shearing, suggesting that the PSD evolution depends mainly on whether the soil volume contracts or expands. The volumetric contraction results mainly from compression of interaggregate pores, and the intra-aggregate PSD or intra-aggregate pores are not affected. In compacted and saturated loess, interaggregate pores are compressed from the larger to the smaller, while in intact loess, the PSD evolution depends on whether the soil yields. This difference arises from different cementations that dominate particle associating in three soils. In intact loess, carbonate cementations that can be damaged by remolding and loading contribute greatly to particle associating. As a result, the stability of a pore is controlled not only by its size but also by carbonate cementations at surrounding particle contacts. Clay cementations that play the dominant role in particle aggregating in compacted loess are resistant to loading; thus, aggregates could not be destroyed by loading and the mechanical responses of compacted loess are in fact interactions among aggregates. Both carbonate and clay cementations can fail under the combined effect of loading and inundation, leading to disintegration of aggregates and turning of the loess structure from the double-structured to the uniform type.

1. Introduction

Loess soils distribute in midlatitude semiarid and arid regions; these soils cover large areas of China, Russia, Europe, North America, and New Zealand [1–4]. Loess soils are known for their open structure, which is characterized by high macroporosity and water-sensitive interparticle bonding [5, 6]. These microstructural characteristics have a great impact on the macroscopic hydromechanical behavior; for example, loess soils may have a strong resistance to deformation at an intact state while being highly compressible upon wetting.

The microstructure of a given soil is neither unique nor fixed; it evolves in response to any change in the stress state. Quantitative characterization of the microstructural evolution is of great importance to interpret the soil macroscopic hydromechanical responses and develop constitutive models taking the structural effect into account. For example, current multiscale approaches for modeling the behavior of unsaturated soils are based on the separation and interaction between different levels of structure [7–9].

Characterization of the microstructural evolution is now focused on the soil fabric (the soil microstructure is a combination of the soil fabric and interparticle bonding according to [10]) because its change is more apparent and relevant to the mechanical and hydraulic properties that are of practical engineering interest. In addition, characterization of the soil fabric is much easier. Among the advanced

techniques used for the soil microstructure characterization (the soil fabric mainly, the same hereinafter), the Mercury intrusion porosimetry (MIP) and scanning electron microscopy (SEM) techniques are the most used [11]. The former is so powerful that can provide quantitative information, that is, pore-size distribution (PSD). The following studies have been carried out using the MIP technique. (i) The PSD was measured after each suction or water content increment to investigate the microstructural evolution during wetting or drying; such studies focused on clayey soils [12–14]. Environmental scanning electron microscope (ESEM) was also used for this purpose. Target relative humidity (or total suction) was imposed directly in the ESEM chamber to moisten or dry the soil specimen; the soil microstructure after the moisture equalization which took a long time was observed [15, 16]. (ii) The PSD was measured after consolidation or shear failure to investigate the microstructural change due to consolidation or shear failure; these studies aimed at a variety of soils [17, 18]. (iii) The PSD was measured after high-temperature heating, soaking in saline solution, leaching, and adding various curing agents to investigate the microstructural change due to heating, salinization, desalinization, and interaction between soil particles and curing agents; these studies also aimed at a variety of soils [19–21]. However, only a few studies have examined the microstructural change of loess due to consolidation, shear failure, or wetting collapse up to now [22–30]. In related studies, the microstructures of loess before and after consolidation, shear failure, or wetting collapse were measured using the MIP or SEM or both techniques and compared. For example, Jiang et al. [22] measured the PSDs of intact and compacted loess before and after triaxial test and concluded that the change occurs to interaggregate pores only and is stress path-dependent. Xie et al. [26] combined the SEM and image processing techniques to analyze the two-dimensional shape features of pores in intact loess after creep test. Li et al. [27] also extracted the two-dimensional shape features of pores and particles in intact and saturated loess after confined compression test using the SEM and image processing techniques. They concluded that pore spaces larger than 60 μm mainly provide spaces for collapse. Luo et al. [25] carried out an end-member model to denote the changes in the pore structure with the macroscopic stress-strain responses of intact loess, based on the pore structure analysis using the SEM and image processing techniques. However, how the microstructure of loess evolves during consolidation, shearing, wetting, drying, heating, and other processes remains unclear.

This paper aims to examine the microstructural evolution of intact, compacted, and saturated loess during deformation associated with consolidation or shearing. The microstructural evolution, the PSD evolution to be more specific, during consolidation is examined by comparing the PSDs of nominally identical loess specimens consolidated to various confining stresses in triaxial cells. Similarly, the PSD evolution during shearing is examined by comparing the PSDs of nominally identical loess specimens consolidated under the same confining stress and then sheared to sequential axial strains. So, the novelty of this study is that the PSD evolution of intact, compacted, and saturated loess during consolidation and shearing is revealed by combining various experimental methods, such as the triaxial testing and MIP technique; the mechanism for the microstructural evolution is interpreted based on measured data and statistical results. The main body of this paper begins with a brief description of the loess microstructure with the micrographs obtained by the SEM technique. Then, the results of the MIP tests are presented; the PSDs of specimens that were brought to different stress states are compared, and the PSD evolution is analyzed for each loess, that is, intact, compacted, and saturated loess. In the end, the mechanism for the PSD evolution is discussed, and the PSDs at the stress states beyond scope of this experimental study are predicted for three loess soils.

2. Material and Methods

2.1. Test Material. Loess from Xi'an, China, was studied for the purpose of examining the microstructural evolution provoked by hydraulic and mechanical loading. Intact block samples of about 10 cm in diameter and 20 cm in height were extracted by hand at a depth of about 5 m in an exploratory well excavated at the sampling site. Physical properties of the loess soil studied are summarized in Table 1. The grain-size distribution shows that this loess is mainly composed of silts (i.e., 0.005–0.075 mm) and clays (<0.005 mm), taking up 82.1% and 15.9% by mass, respectively. This loess is clayey loess, according to the loess classification proposed by Gibbs and Holland [31] based on plasticity index and liquid limit, as shown in Figure 1. The mineral composition of the loess soil studied characterized by the X-ray diffraction (XRD) technique is presented in Table 2.

2.2. Test Program. Consolidated drained (CD) triaxial tests were conducted on intact, compacted, and saturated loess specimens of 39.1 mm in diameter and 80 mm in height. Intact specimens were extracted from block samples. Saturated specimens were obtained by immersing intact loess specimens in deaired water under vacuum condition to achieve a degree of saturation greater than 95%. Disturbed soils were air-dried for several days, pulverized with a rubber mallet, sieved with a 0.25 mm sieve, and moistened with deaired water to reach a predesigned water content (close to the in situ water content). After the moisture equalization, wet soils were compacted to a density close to the in situ density to obtain compacted specimens. Compaction was conducted in a mold of 39.1 mm in diameter in three layers with scarification between layers to ensure homogeneity of the soil specimen. These loess specimens were then loaded in triaxial cells. In each CD test, the specimen was first consolidated to predetermined confining stress. Consolidation was assumed to be completed as the readings of axial displacement maintained constant. The specimen was then sheared under drained condition by increasing the deviator stress at a constant strain rate (i.e., 0.012% per minute) to a predetermined axial strain. The microstructure of each specimen after the triaxial test was characterized using the MIP technique. The stress paths for the triaxial drained tests

Table 1: Physical properties of the studied loess soil.

Sampling site	In situ water content w (%)	In situ density ρ (mg/m^3)	Specific gravity G_s	Atterberg limits (%)			Classification
				Liquid limit w_L	Plastic limit w_P	Plasticity index I_P	
Xi'an	15.0–20.0	1.44–1.68	2.70	34.2	18.6	15.6	Clayey loess

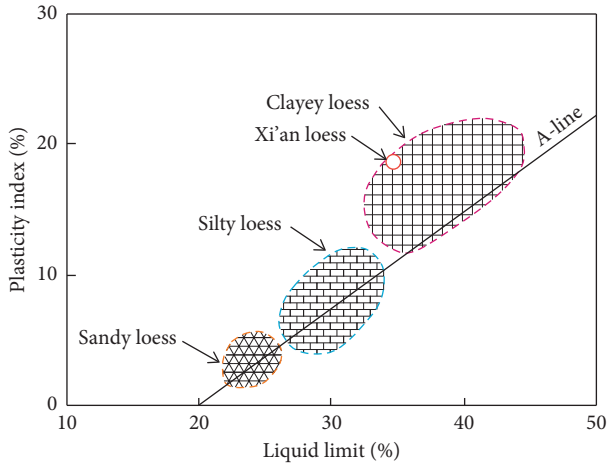

Figure 1: Plasticity chart showing the classification of the studied loess soil.

Table 2: Mineralogical composition of the studied loess soil.

Mineral	Quartz	Plagioclase	Potash feldspar	Calcite	Dolomite	Illite	Chlorite	Amphibole	Hematite
Content (%)	52.0	13.6	3.4	11.0	1.6	8.0	8.5	1.4	0.5

are plotted in the confining stress (p) versus deviator stress (q) plane in Figure 2; each circle represents a stress state at which the PSD was measured.

(1) Specimens were consolidated to different confining stresses, that is, 100, 200, 300, and 400 kPa. When the specimen was no longer deformed, the test was terminated and the specimen was taken out from the triaxial cell. A cubic specimen was trimmed out from each specimen, at about 1/3 specimen height, and used for the MIP test. The PSDs of deformed specimens were compared to interpret the PSD evolution induced by consolidation (isotropic loading).

(2) Under each confining stress (i.e., 100, 200, 300, or 400 kPa), up to four specimens were sheared to a sequence of axial strains, that is, 5%, 10%, 15%, and 20%. As the target axial strain was reached, the test was ceased and the specimen was taken out from the triaxial cell. Similarly, a cubic specimen was prepared for the MIP test. The PSD change in response to any increment of axial strain during shearing (anisotropic loading) can be derived by comparing the PSDs before and after the axial strain increment.

To conduct a MIP test, each cubic specimen was mildly air-dried [32]. A porosimeter that can apply an intrusion pressure ranging between 0.5 and 60,000 psi was used; the

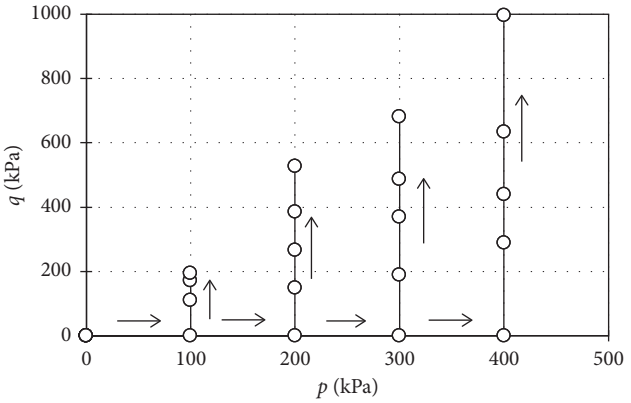

Figure 2: Stress paths of the triaxial tests on intact, compacted, and saturated loess specimens (each circle represents a stress state at which the PSD was measured).

corresponding entrance diameter ranges from 3.0 to 360,000 nm according to Laplace's capillarity law. The pores with an entrance diameter beyond this range will not be intruded. In addition, the isolated pores and the constricted pores only accessible through the channels that are too small to be intruded (less than 3.0 nm) will not be intruded [23]. It is, therefore, understandable that the cumulative intrusion void ratio, e_{in}, is typically lower than the void ratio determined by conventional approach, e. Figure 3 compares the e

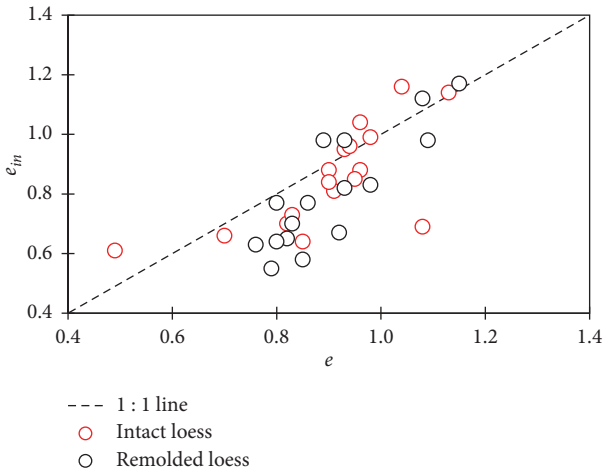

Figure 3: Comparison between e_{in} and e.

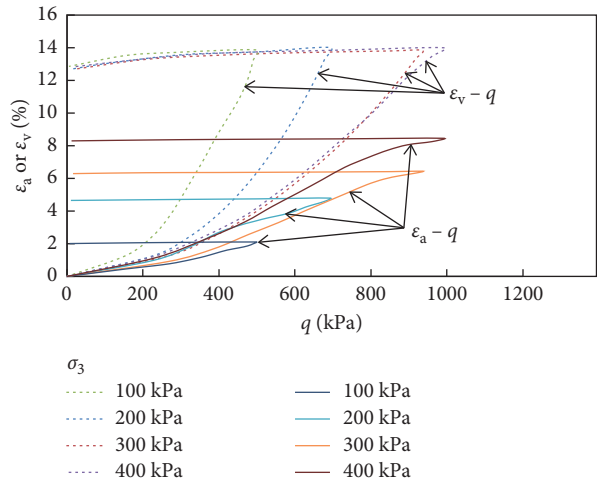

Figure 4: Stress-strain curves of intact loess specimens during anisotropic loading-unloading process.

values with the e_{in} values of a total of 33 intact and compacted loess specimens. It can be seen that in most cases e_{in} is lower than e. With regard to the cases in which e_{in} is greater than e, that is probably because of sample disturbance and technical or operational error during the measurement. Since a single technique (i.e., MIP) was used and the changes instead of the absolute values were concerned, this method was thought to be reliable to reveal the microstructural evolution induced by specimen-scale deformation.

It is worth noting that the PSDs were measured on the specimens unloaded. Consequently, the results can only indicate the influence of plastic deformation on the soil fabric. For the three loess soils studied, recoverable volume changes during shearing were found to be very small even under low confining stress. Take intact loess as an example; the stress-strain curves during the loading-unloading paths are summarized in Figure 4, where ε_v is the volumetric strain, ε_a is the axial strain, q is the deviator stress, and σ_3 is the confining stress.

3. Results

3.1. Microstructural Characteristics of Loess Soils. Loess soils are mainly composed of silts, with a fraction between 60% and 90%. Clays (<0.005 mm) can account for 5% to a maximum of 30% of the total solid mass; they are functioning as aggregates rather than individuals [33]. Aggregates are associations of soil particles (i.e., clays, silts, and sands). In each loess soil studied (intact, compacted, or saturated), aggregates dominate the soil structure; see Figure 5. In comparison with intact loess, aggregates in compacted loess have greater sizes; however, aggregates in saturated loess are smaller than that in intact loess. In intact loess, after the wind-blown dust and sand settled, calcium ions produced by leaching of primary calcites can react with carbonate ions, leading to illuviation of secondary calcites which wrap and cover solid particles like films. So, association of particles in intact loess is mainly attributed to carbonate cementations, also due to clay cementations. There also have soluble and insoluble salts, such as sodium chloride and calcium sulfate, their contribution is limited because of the low contents. However, carbonate cementations would experience irreversible damage during remolding due to crushing or pulverizing. So, in compacted loess, formation of aggregate is mainly due to surface charges of clay minerals, van der Waals attraction, and matric suction [34]. Considering the elemental role of aggregates in loess soils, the pores are thought to be of two sets: intra-aggregate pores (or micropores) and interaggregate pores (or macropores). That is to say, these soils are double-structured and have a bimodal PSD, which can be regarded as the superposition of two unimodal PSDs: one is for intra-aggregate pores and the other is for interaggregate pores; $e_{in} = e^s + e^L$, where e^s and e^L are the cumulative intrusion void ratios for intra-aggregate pores and interaggregate pores, respectively. On each unimodal PSD, the peak density corresponds to the dominant pore diameter, d_{micro} or d_{macro}. The delimitation of two unimodal PSDs corresponds to the delimiting pore diameter, $d_{delimiting}$, which depends on the grain-size distribution and the method used to determine the PSD [15, 16].

3.2. PSDs of Intact, Compacted, and Saturated Loess. Figure 6 compares the PSDs of intact loess, compacted loess with identical dry densities or void ratios (i.e., 1.15), and saturated loess, including cumulative curves and density curves in semilogarithmic scales. First of all, it is noteworthy that the drop in the density for the entrance pore diameter between 4 and 7 μm, as highlighted in the green-colored oval in Figure 6(b), might be due to experimental error associated with the transition of two pressure units during the intrusion of Mercury.

In Figure 6(a), it is shown that inundating intact loess leads to a great reduction in e_{in} (i.e., 1.11 and 0.69 for intact and saturated loess specimens, resp.), which provides evidence for the self-weight collapsibility of intact loess since the specimen was soaked without loads. Other proofs are in Figure 6(b), the larger density of the pores between 5.3 and

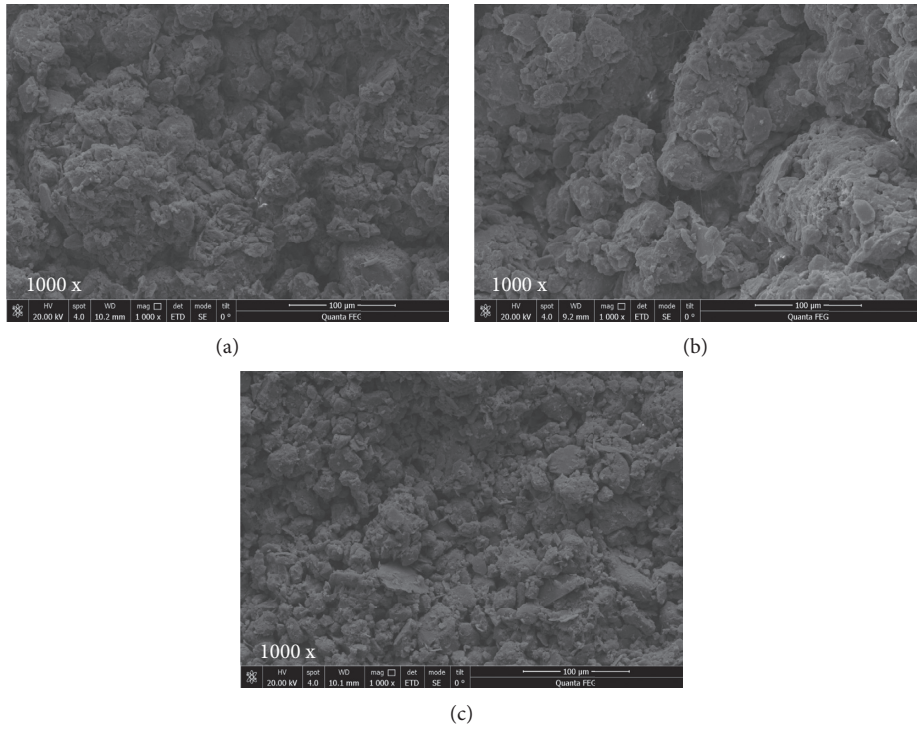

Figure 5: Micrographs of (a) intact, (b) compacted, and (c) saturated loess.

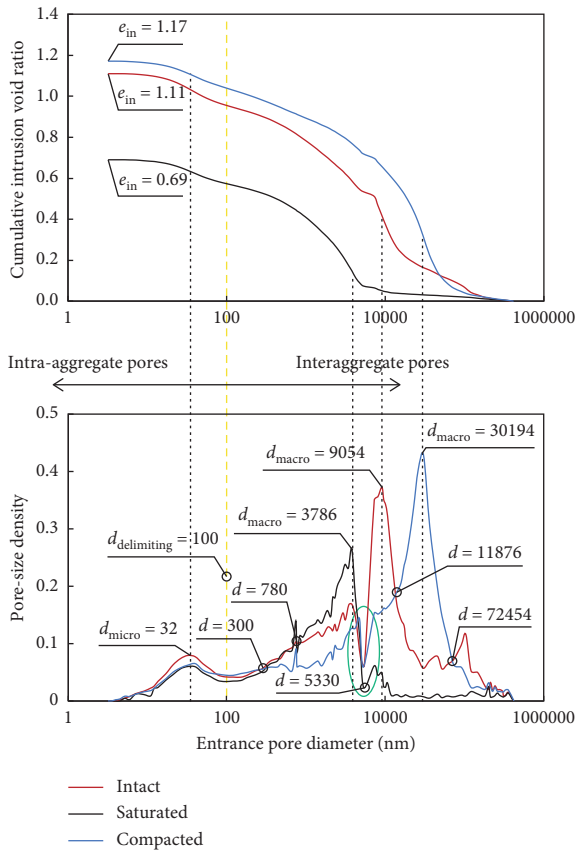

Figure 6: PSDs of intact, compacted, and saturated loess specimens.

360 μm and the lower density of the pores between 0.8 and 3.8 μm in intact loess than those in saturated loess. It means that the pores between 5.3 and 360 μm in intact loess collapsed when specimen was inundated, transforming into smaller ones with an entrance diameter between 0.8 and 3.8 μm. From Figure 6(b), it is shown that three soils almost have the same d_{micro}, of about 40 nm, and similar densities for the pores smaller than 0.3 μm, which indicates that inundating and remolding have little impact on small pores ($\leq$0.3 μm), including intra-aggregate pores ($\leq$0.1 μm). Although from the micrographs aggregates are seen to have different sizes in three soils (Figure 5), their PSDs for intra-aggregate pores are similar. It should be noted that the electric double layer on the surfaces of particles can be thickened with increase of soil water content, leading to weakening of interparticle bonding and swelling of aggregates, bearing in mind that swelling or shrinking of aggregates due to wetting or drying is reversible [8]. In addition, the cubic specimen was mildly air-dried before the measurement of PSD; the test results could not reflect the changes in aggregate fabric and intra-aggregate pores.

Intact loess has more pores between 0.3 and 11.9 μm; compacted loess has more pores between 11.9 and 72.5 μm. In addition, two soils have quite different d_{macro}. That is because aggregates in compacted loess are greater than that in intact loess; as a result, interaggregate pores in compacted loess are larger than that in intact loess. Particularly, compacting a clayey soil at drier side of the optimum (the case here) facilitates the development of aggregates with greater dimensions [34]. However, a firm conclusion on the PSD change due to remolding cannot be drawn upon the comparison of PSDs of intact loess and a single compacted specimen since molding water content has a great influence on the type of structure (i.e., aggregated, dispersed, or flocculated) and aggregate-size distribution of compacted loess. The PSDs of intact and compacted loess were once compared by Wen and He [20]; Jiang et al. [22]; Ng et al. [23]; Shao et al. [24]; and Wang et al. [35]. Wen and He [20] tested six loess soils, while most of them (both intact and compacted) have a unimodal PSD, which may be related to the settings of porosimeter. So, their test results are not considered. In some of the studies [22, 35], the intra-aggregate PSDs (for intra-aggregate pore series) of intact and compacted loess are similar, while in the others [23, 24], the intra-aggregate PSD changed significantly after remolding. Compacted specimens in the above four studies were prepared at 16.9%, 18%, 10.9%, and 9.9% to a dry density between 1.23 and 1.5 g/cm^3; the former two were close to the optimum water contents, while the latter two were smaller than the optimum water contents. A review of these test results also cannot reach a firm conclusion; however, it can be inferred that the optimum water content corresponds to the minimum amount of water required for the development of a complete electric double layer. When compacted at the optimum water content or greater, compacted soil would have a certain intra-aggregate pore series, while when compacted at dry side of the optimum condition, the intra-aggregate PSD varies with molding water content.

3.3. PSD Evolution during Consolidation. The PSD evolution during consolidation (or isotropic loading) is depicted in Figure 7–9for intact, saturated, and compacted loess by comparing the PSDs of nominally identical specimens consolidated to different confining stresses. It is found that intra-aggregate pores (<0.1 μm) are unaffected in all three soils (intact, saturated, and compacted loess). In Figure 7, a slight decrease in d_{macro} is observed with increase of confining stress. In comparison, the density of the pores greater than 10 μm reduces a lot when confining stress increases from 200 to 300 kPa, which corresponds to a remarkable reduction in e_{in}. This range happens to contain the stress at the maximum curvature of e-log$p$ curve. The stress at the maximum curvature can be termed structural yield stress, which is the sum of preconsolidation stress and structural strength of intact loess [36, 37]; the former ranges between 85 and 135 kPa for the studied intact loess; the latter refers to the contribution of interparticle carbonate cementations to the compressive strength [38]. When intact loess is subjected to a stress greater than its structural yield stress, the soil structure will alter due to bonding breakage and the soil specimen will undergo significant volumetric contraction; otherwise, the soil structure will remain intact in principle. Therefore, it is the interparticle carbonate cementations in intact loess that resist the overburden stress exceeding the preconsolidation stress. For saturated loess, most of the pores larger than 5 μm are closed even without load, suggesting that the structural strength is reduced significantly as intact loess is inundated. A noticeable transformation of the pores between 2 and 4 μm into smaller pores between 0.5 and 2 μm takes place when confining stress increases to 300 kPa; otherwise, the PSD changes induced by increase of confining stress are very small for saturated loess; see Figure 8.

The PSD evolution of compacted loess is more regular, as shown in Figure 9. A distinct reduction in e_{in} is produced, and this reduction is mainly attributed to decrease of the interaggregate pores with an entrance diameter greater than 6 μm. For example, turning of the pores greater than 18.2 μm into the pores between 6 and 18.2 μm is induced as compacted loess is subjected to confining stress of 100 kPa. In response to the subsequent increase of confining stress, the density of interaggregate pores decreases and d_{macro} moves towards lower values. In short, interaggregate pores in compacted loess are compressed from the larger to the smaller. It means the vulnerability of a pore in compacted loess is related to its size only.

3.4. PSD Evolution during Shearing. The PSD evolution during shearing (or anisotropic loading) is analyzed by comparing the PSDs of nominally identical specimens that were consolidated to the same confining stress and then sheared to a sequence of axial strains. Before putting forward the analysis of the PSD evolution, it should be pointed out that all of the stress-strain curves show strain hardening that is associated with volumetric contraction. And in fact, all of the specimens (intact, compacted, or saturated) contracted throughout the test (the volumetric strains were always positive); radial dilation took place at a lower rate than the

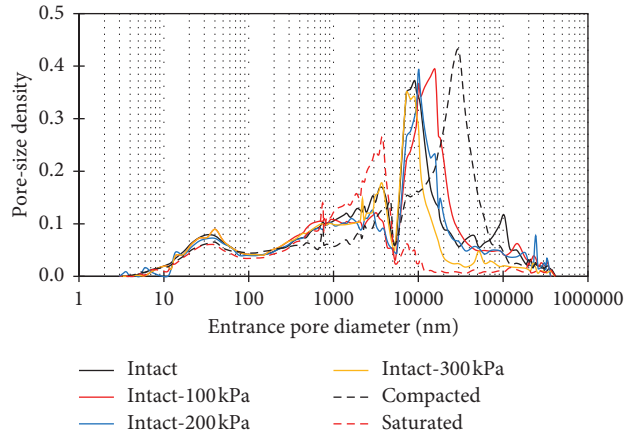

Figure 7: PSDs of intact loess specimens consolidated to various confining stresses.

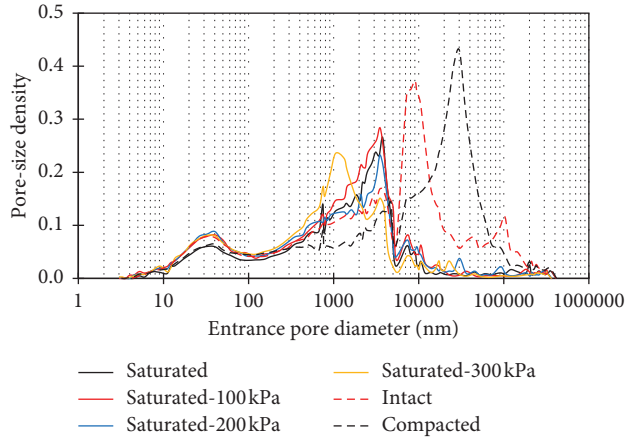

Figure 8: PSDs of saturated loess specimens consolidated to various confining stresses.

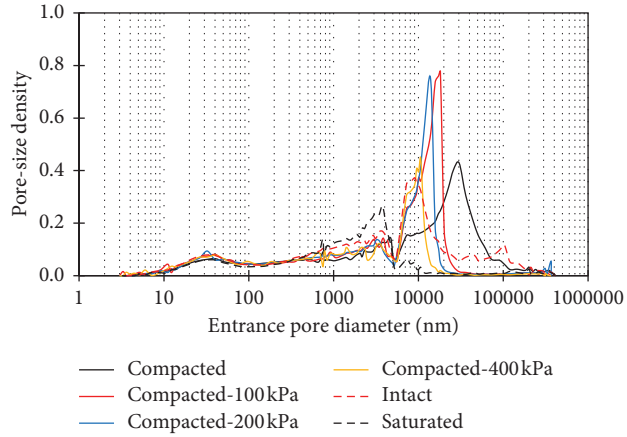

Figure 9: PSDs of compacted loess specimens consolidated to various confining stresses.

accumulation of axial displacement. Since all of the stress-strain curves show strain hardening, the critical state is thought to be achieved at 15% axial strain and the critical state lines (CSLs) are drawn in Figures 10(b), 10(e), and 10(h). The slope and intercept of the CSL, M, and μ, can be obtained, upon which the effective internal friction angle and effective cohesion, φ and c, are determined ($\varphi = \sin^{-1}[3M/(6+M)]$, $c = \mu\ (3-\sin\varphi)/(6\cos\varphi)$). In addition, the intersection of the CSL and p axis is termed the bonding stress, σ_0, which is related to the degree of saturation and interparticle bonding [39]. These parameters are summarized in Table 3. Intact loess has much greater c and σ_0 than compacted loess and saturated loess, meaning that it has much stronger interparticle bonding.

Figures 11–13 present the PSDs of intact, compacted, and saturated loess specimens sheared to sequential axial strains under confining stresses of 200 and 400 kPa. Each curve is named X–m – n%, where X denotes the loess soil, intact (I), compacted (C), or saturated (S); m denotes the confining stress and n denotes the axial strain. For intact loess, as the axial strain augments and the specimen contracts under the increasing deviator stress, the PSD for intra-aggregate pores (<0.1 μm) still remains unchanged even if the specimen is sheared to an axial strain of 20% under confining stress of 400 kPa. Interaggregate pores are compressed before all larger pores are closed during shearing at the confining stress of 200 kPa. That is because as aforementioned the soil structure remains intact after consolidated to 200 kPa; the interparticle carbonate cementations around some interaggregate pores do not fail and can still resist increase in deviator stress. For this reason, the pore stability in intact loess is dependent not only on the pore size but greatly on surrounding interparticle carbonate cementations. For example, root channels with the walls well filmed with calcium carbonates would not be closed even if the soil specimen suffers significant volumetric contraction [32]. This statement is evidenced by Figure 11(b); confining stress of 400 kPa is high enough to break most interparticle carbonate cementations in intact loess, so shearing activates the particle movement and rotation, resulting in turning of larger pores into smaller pores and removal of almost all large pores (≥5 μm) when reaching the critical state, such as I–400–15% and I–400–20%.

As for compacted loess, after specimen is consolidated to a given confining stress, proceeding of shearing causes compression of interaggregate pores, from the larger to the smaller. For this reason, reduction in the density of larger pores is accompanied by growth in the density of smaller pores, indicating the transformation of larger pores into smaller pores. When all of the pores with an entrance diameter greater than d_{macro} are compressed, further volumetric contraction of the specimen leads to a reduction in d_{macro}. The PSD thus exhibits a drop at d_{macro}. It can be seen from the curves under the confinement with a stress level no more than 400 kPa; the pores smaller than about 1 μm were not disturbed by shearing. The decrease of e_{in} is attributed largely to compression of the pores greater than 1 μm.

The PSD evolution of saturated loess during shearing is similar to that of compacted loess. To be more specific, interaggregate pores are compressed from the larger to the smaller; compression of larger pores typically results in an increase in the density of smaller pores. It is shown that very

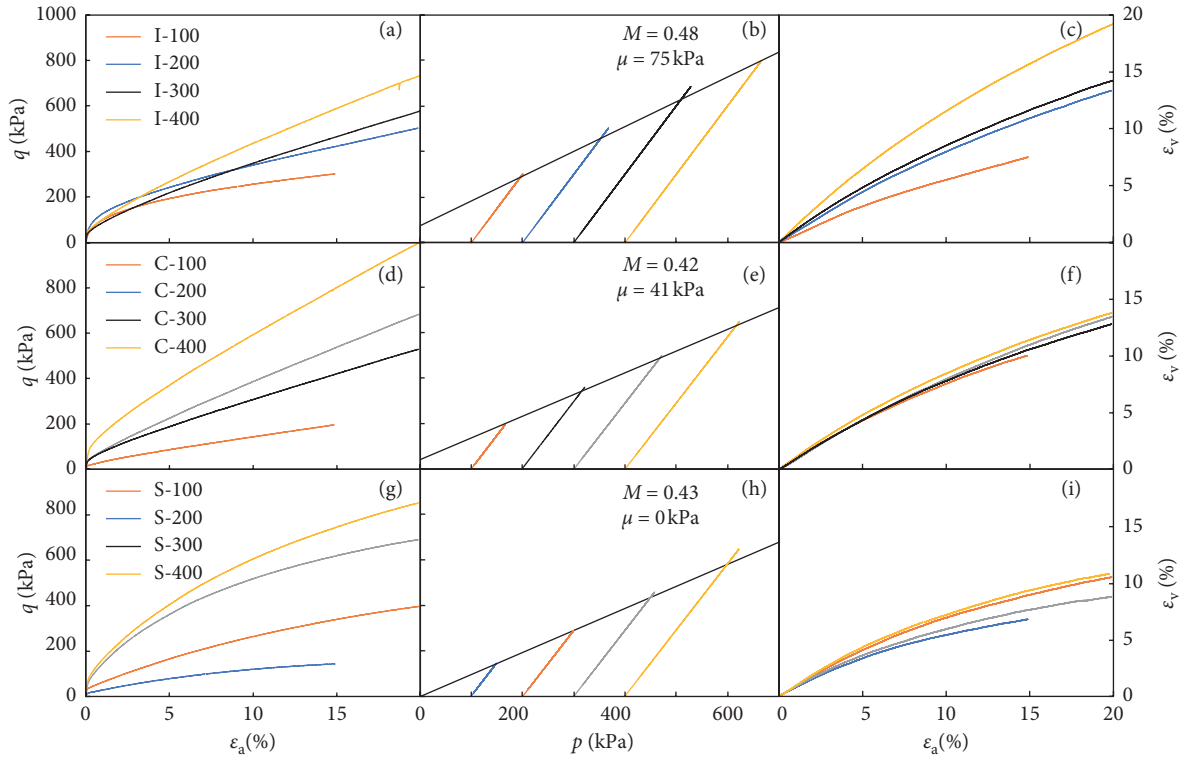

Figure 10: Results of triaxial drained tests on intact, compacted, and saturated loess specimens (q is the deviator stress, kPa; p is the confining stress, kPa; ε_a is the axial strain, %; ε_v is the volumetric strain, %).

Table 3: Parameters of the critical state.

Loess	M	μ (kPa)	φ (°)	c (kPa)	σ_0 (kPa)
Intact	0.48	75	12.9	36	68
Compacted	0.42	41	11.4	20	34
Saturated	0.43	0	11.6	0	0

M and μ are the slope and intercept of the critical state line (CSL); φ and c are the effective internal friction angle and effective cohesion; σ_0 is the bonding stress.

little change happens to the PSD for intra-aggregate pores. However, it can be seen from Figure 13(b) that the density of the pores around $d_{\text{delimiting}}$ (i.e., 0.1 μm) has a potential to increase as a result of diminishing of larger pores, which suggests that the bimodal PSD may be modified to be unimodal as the specimen contracts further.

3.5. Variations of the PSD Parameters. Knowing $d_{\text{delimiting}}$, e^L and e^s can be determined from the PSD in terms of cumulative intrusion void ratio and are presented with respect to e_{in} in Figures 14(a) and 14(b). The linear relationship between e^L and e_{in} shown in Figure 14(a) and the almost constant e^s shown in Figure 14(b) provides strong evidence for the PSD evolution of loess soils stated above that the contraction of soil specimen or reduction in e_{in} is mainly due to compression of interaggregate pores. It is worth noting that all intact, compacted, and saturated specimens have almost the same value of e^s, that is, 0.17. In the studies by Jiang et al. [22] and Wang et al. [35]; intact and compact loess soils were reported to have the same e^s; e^s is 0.15 in the former study and 0.13 in the latter. Another difference among three compacted loess soils tested by Jiang et al. [22]; Wang et al. [35], and in this study is the clay content, that is, 4.8%, 9.8%, and 15.9%, respectively. It has already highlighted that the intra-aggregate PSD is greatly controlled by molding water content. Besides, the intra-aggregate PSD and e^s are of course related to the granular and mineral composition of soil material. Under such a scenario, the dependency of e^s on molding water content suggested by Romero et al. [40]for compacted clayey soils cannot be determined with certainty for the studied compacted loess because the influence of clay content and the difference arising from test settings cannot be excluded.

The relationship between d_{micro} and e_{in} of compacted and saturated loess in a semilogarithmic scale is more linear than that of intact loess; see Figure 14(c). That is because in compacted and saturated loess, interaggregate pores are compressed from the larger to the smaller as the specimen contracts. When the pores with an entrance diameter greater than d_{macro} are all compressed, further volumetric contraction can certainly lead to a reduction in d_{macro}. With regard to intact loess, d_{macro} generally decreases with decrease of e_{in}, while its variation is more random than that of the other two loess soils. As stressed before, macropores with surrounding particles well cemented with carbonate cementations in intact loess can only fail under quite high-stress states, which prevents d_{macro} from quick reducing with increase of load increase.

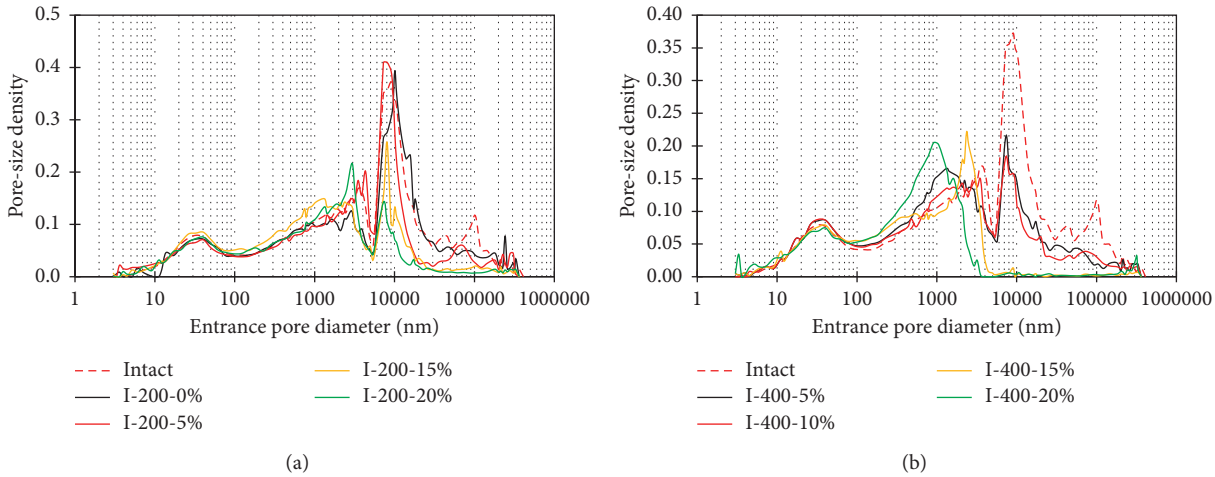

Figure 11: PSDs of intact loess specimens sheared to sequential axial strains under the confining stress of (a) 200 kPa and (b) 400 kPa.

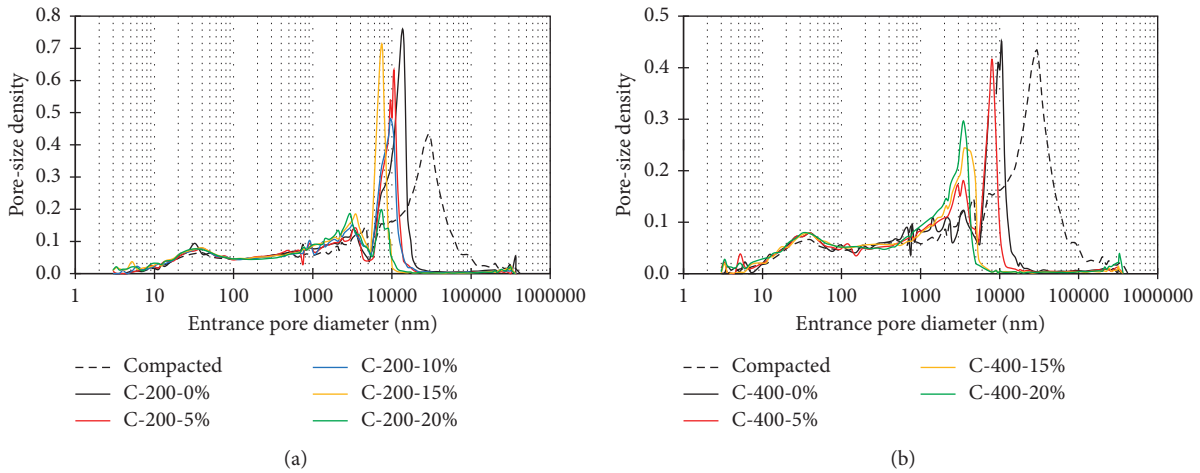

Figure 12: PSDs of compacted loess specimens sheared to sequential axial strains under the confining stress of (a) 200 kPa and (b) 400 kPa.

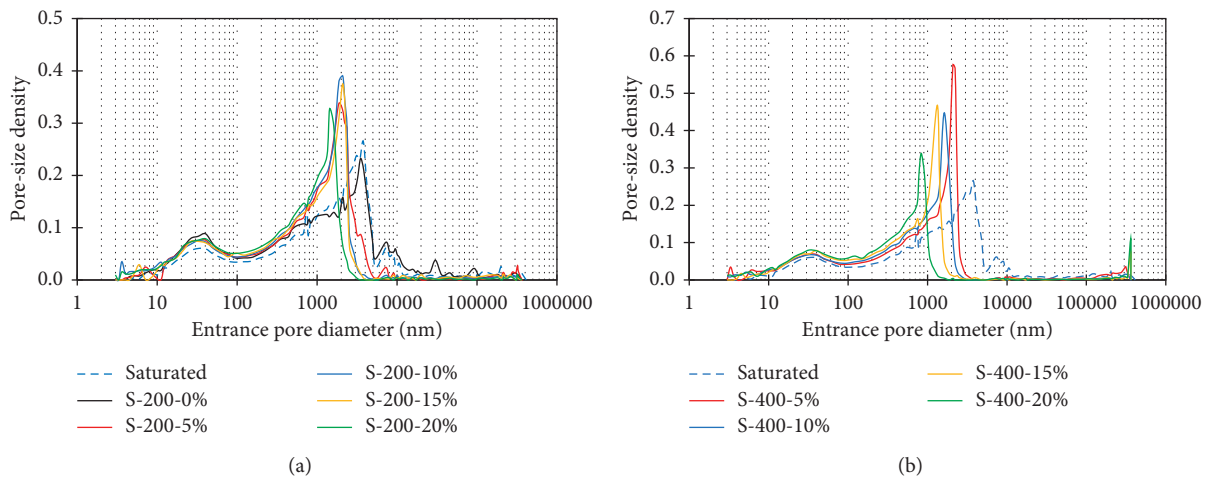

Figure 13: PSDs of saturated loess specimens sheared to sequential axial strains under the confining stress of (a) 200 kPa and (b) 400 kPa.

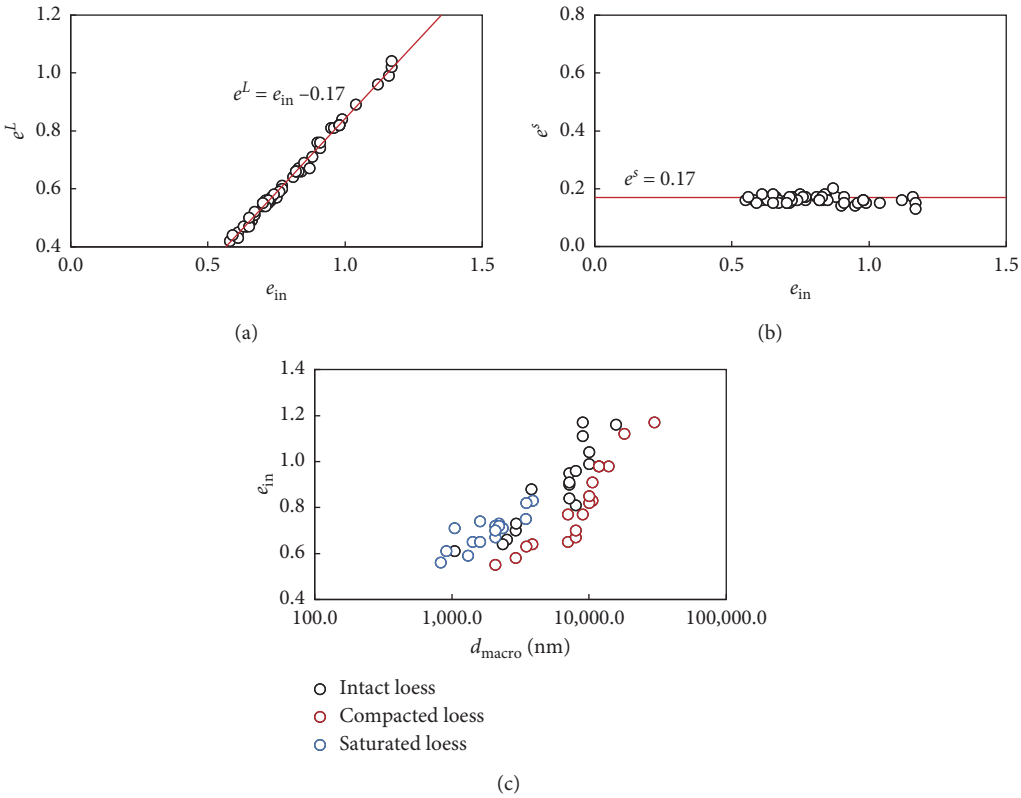

Figure 14: Relationship between (a) e_{in} and e^L; (b) e_{in} and e^s; (c) d_{macro} and e_{in}.

4. Discussion

The loess soils studied in the present study are highly contractive, all of the loess specimens showed strong volumetric contraction in the triaxial tests (Figure 10). The PSD evolution induced by consolidation is similar to that induced by shearing. It thus can be stated that the PSD evolution mainly depends on whether the soil volume contracts or expands. This conclusion can also be drawn from the test results of Luo et al. [25]. Since the stress-strain curve exhibits strong strain hardening, the specimen may contract a little further in response to further increase in shear stress. However, intra-aggregate pores in compacted loess would not be affected under any loading condition (consolidation or shearing), even if the soil is in the densest state [35]. In compacted loess, intra-aggregate pores are formed as dry soil is mixed with water and moisture homogenization throughout the soil is reached, that is, formation of aggregates. It indicates that aggregates in compacted loess could not be destroyed due to loading, irrespective of the stress path, and the mechanical responses of compacted loess are the interactions among aggregates rather than among particles. That is because clay minerals (illite and chlorite) that play a dominant role in aggregating particles in compacted loess are vulnerable to wetting while they are resistant to loading. For this reason, the double-structured characteristic of compacted loess could not be eliminated (Figure 15(b)).

Similarly, the bimodal PSD of intact loess could not be eliminated, while it might be weakened if the specimen contracts further. With regard to the mechanism, as mentioned earlier, particles in intact loess are cemented with carbonate cementations and clay cementations. Carbonate cementations can be damaged by remolding, loading, and leaching [41]. For this reason, aggregates in intact loess could be destroyed due to loading, while not completely, because the aggregates formed due to the surface charges of clay minerals and various attractions between clay particles could not be destroyed, similar to that in compacted loess. In addition, it is difficult for the particle connections that are strongly cemented with calcium carbonates to fail. Under such a scenario, aggregates in intact loess could not be completely destroyed, and the bimodal nature of the PSD could not be eliminated but could be weakened (see Figure 15(a)).

However, both carbonate cementations and clay cementations can fail under the combined effect of loading and inundation, leading to disintegration of particle associations [27, 41], which is evidenced by the zero values of c and σ_0 (Table 3). Bear in mind that the soil specimen was saturated before conducting the triaxial test and the test took a long time because of the drained condition; thereby, carbonate cementations could be weakened and damaged a little. This reasoning is supported by the finding that the vulnerability of pores in saturated loess is mainly controlled by the pore size and that the density for the entrance diameter around $d_{delimiting}$ (0.1 μm) shows a potential to increase as a result of

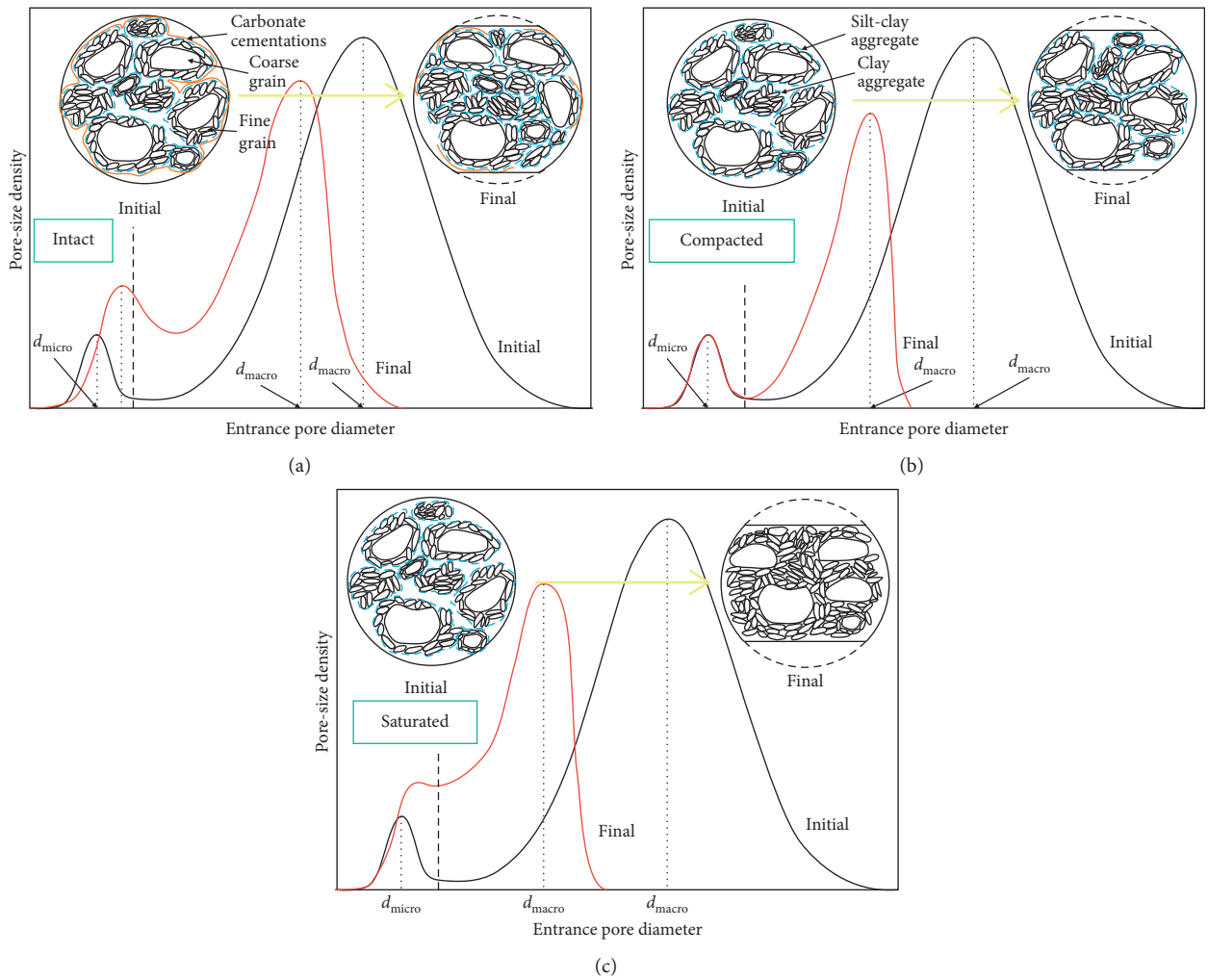

Figure 15: Predicted PSD evolution of (a) compacted loess; (b) intact loess; (c) saturated loess.

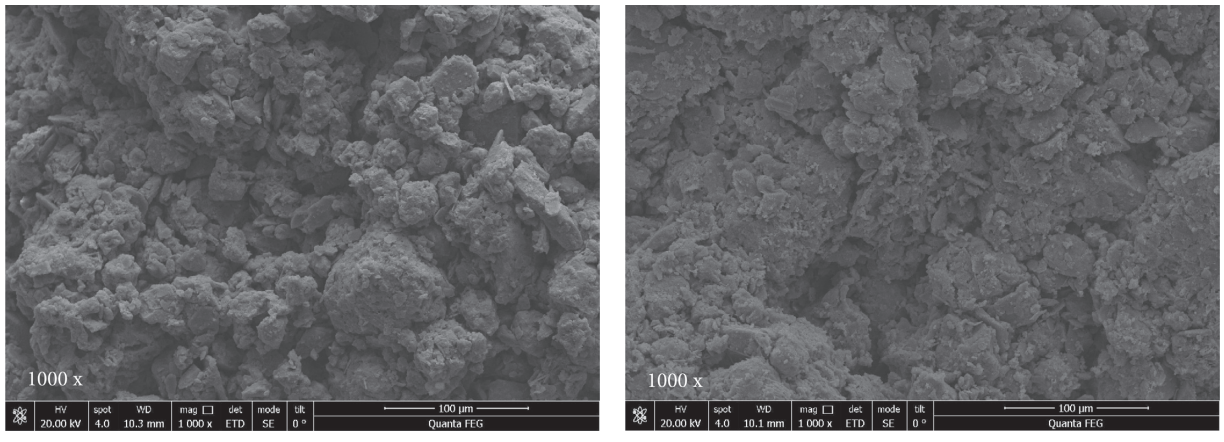

Figure 16: Continued.

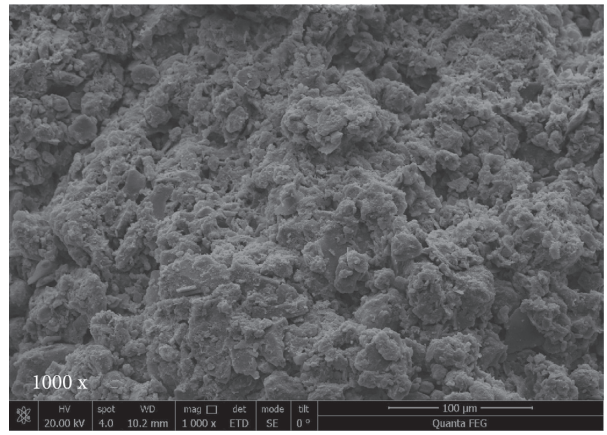

(c)

Figure 16: Micrographs of loess specimens after the triaxial tests. (a) I-300-0%. (b) C-400-20%. (c) S-300-10%.

the diminishing of larger pores when saturated specimen was sheared to 20% axial strain under 400 kPa (Figure 13(b)). Clay minerals in the studied loess are illite and chlorite in essence; they all have a double-layer structure, large specific surface area, and strong hygroscopic property with the layered crystal structure. When water is accessible, water molecules fill the interlayer spaces, leading to expansion of the crystal structure and sharp decline of the structural strength. For this reason, considering that the studied loess is well-grained (coefficient of uniformity, $C_u \geq 5$; coefficient of curvature, $C_c = 1–3$), the microstructure of saturated loess is thought of turning to be uniform and the PSD would turn to be unimodal if the specimen contracts further during shearing (Figure 15(c)).

The above reasoning is also supported by the micrographs taken on the specimens after the triaxial tests. Figure 16(b) shows the microstructure of the specimen C-400-20%, which experienced the largest volumetric contraction among all compacted specimens. Even so, aggregates can still be clearly identified; the contact area between aggregates is enlarged with increase of soil compactness. The microstructure of the specimen I-300-0% is shown in Figure 16(a), in which aggregates are much smaller than that in compacted loess. However, the microstructure of saturated specimen is getting uniform due to loading and aggregates cannot be identified because of the vague outlines; see Figure 16(c).

5. Conclusions

The microstructure of soil has great control on the hydromechanical behavior and it evolves in response to any change in the stress state. Although a few studies have examined the changes of the loess soil microstructure due to consolidation, shear failure, and wetting collapse, how the loess soil microstructure evolves along these stress paths remains unclear. The present study examines the PSD evolution of intact, compacted, and saturated loess in triaxial tests by comparing the PSDs of nominally identical specimens consolidated to different confining stresses or sheared to sequential axial strains under the same confining stress. Some important conclusions can be drawn upon this integrated experimental study.

The studied loess soils (intact, compacted, and saturated) are highly contractive; all loess specimens showed strong volumetric contraction during loading, either isotropic or anisotropic. The PSD evolution during consolidation is similar to that during shearing, suggesting that the PSD evolution depends mainly on whether the soil volume contracts or expands. The intra-aggregate PSD or intra-aggregate pores (<0.1 μm) are not affected within the stress level applied. The volumetric contraction results mainly from compression of interaggregate pores. Reduction in the density of larger interaggregate pores is typically accompanied by growth in the density of smaller interaggregate pores, suggesting that a transformation of larger pores into smaller pores is induced by loading. In compacted and saturated loess, interaggregate pores are compressed from the larger to the smaller; it means the pore stability depends mainly on the pore size, while in intact loess, the stability of a pore is controlled not only by its size but also by carbonate cementations at surrounding particle contacts, and the PSD evolution depends on whether the soil yields.

Aggregates in compacted loess could not be destroyed by loading, irrespective of the stress path, since clay minerals that play the dominant role in aggregating particles in compacted loess are resistant to loading. The double-structured characteristic of compacted loess thus could not be eliminated, and the bimodal nature of the PSD could not be eliminated. The mechanical responses of compacted loess are the interactions among aggregates rather than among particles. While the bimodal nature of the PSD of intact loess could be weakened because carbonate cementations that contribute greatly to particle associating could be weakened and damaged by loading. The microstructure of saturated loess is thought of turning to be uniform as a result of disintegration of aggregates because the cementations, both clay minerals and calcium carbonates, can fail under the combined effect of loading and inundation. The PSD would turn to be unimodal if saturated loess specimen contracts

further. The reasoning based on the comparison of PSDs is supported by the soil macroscopic responses and microscopic observations.

Data Availability

The data used to support the findings of this study are available from the corresponding author upon request.

Conflicts of Interest

The authors declare that they have no conflicts of interest.

Acknowledgments

The authors acknowledge the funding received from the National Natural Science Foundation of China (42007251; 11572245), the China Postdoctoral Science Foundation (2019M653883XB), and the Shaanxi Key Laboratory of Loess Mechanics and Engineering (LME201803).

References

[1] E. Derbyshire and T. W. Mellors, "Geological and geotechnical characteristics of some loess and loessic soils from China and Britain: a comparison," *Engineering Geology*, vol. 25, no. 2–4, pp. 135–175, 1988.

[2] E. A. C. Costantini, S. Carnicelli, D. Sauer et al., "Loess in Italy: genesis, characteristics and occurrence," *Catena*, vol. 168, pp. 14–33, 2018.

[3] H. Sadeghi, M. Kiani, M. Sadeghi, and F. Jafarzadeh, "Geotechnical characterization and collapsibility of a natural dispersive loess," *Engineering Geology*, vol. 250, pp. 89–100, 2019.

[4] K. Yates, C. H. Fenton, and D. H. Bell, "A review of the geotechnical characteristics of loess and loess-derived soils from Canterbury, South Island, New Zealand," *Engineering Geology*, vol. 236, pp. 11–21, 2018.

[5] P. Li, S. Vanapalli, and T. Li, "Review of collapse triggering mechanism of collapsible soils due to wetting," *Journal of Rock Mechanics and Geotechnical Engineering*, vol. 8, no. 2, pp. 256–274, 2016.

[6] Q. Y. Mu, C. Zhou, and C. W. W. Ng, "Compression and wetting induced volumetric behavior of loess: macro- and micro-investigations," *Transportation Geotechnics*, vol. 23, Article ID 100345, 2020.

[7] A. Gens and E. E. Alonso, "A framework for the behaviour of unsaturated expansive clays," *Canadian Geotechnical Journal*, vol. 29, no. 6, pp. 1013–1032, 1992.

[8] E. Romero, A. Gens, and A. Lloret, "Water permeability, water retention and microstructure of unsaturated compacted Boom clay," *Engineering Geology*, vol. 54, no. 1-2, pp. 117–127, 1999.

[9] E. E. Alonso, N. M. Pinyol, and A. Gens, "Compacted soil behaviour: initial state, structure and constitutive modelling," *Géotechnique*, vol. 63, no. 6, pp. 463–478, 2013.

[10] J. K. Mitchell and K. Soga, *Fundamentals of Soil Behavior*, Wiley, Hoboken, NJ, USA, 2005.

[11] E. Romero and P. H. Simms, "Microstructure investigation in unsaturated soils: a review with special attention to contribution of mercury intrusion porosimetry and environmental scanning electron microscopy," *Geotechnical and Geological Engineering*, vol. 26, no. 6, pp. 705–727, 2008.

[12] G. Della Vecchia, A.-C. Dieudonné, C. Jommi, and R. Charlier, "Accounting for evolving pore size distribution in water retention models for compacted clays," *International Journal for Numerical and Analytical Methods in Geomechanics*, vol. 39, no. 7, pp. 702–723, 2015.

[13] X. Liu, O. Buzzi, S. Yuan, J. Mendes, and S. Fityus, "Multiscale characterization of retention and shrinkage behaviour of four Australian clayey soils," *Canadian Geotechnical Journal*, vol. 53, no. 5, pp. 854–870, 2016.

[14] Z. S. Li, F. E. M. Derfouf, A. Benchouk, N. Abou-Bekr, S. Taibi, and J. M. Fleureau, "Volume change behavior of two compacted clayey soils under hydraulic and mechanical loadings," *Journal of Geotechnical and Geoenvironmental Engineering*, vol. 144, no. 4, Article ID 04018013, 2018.

[15] C. Airò Farulla, A. Ferrari, and E. Romero, "Volume change behaviour of a compacted scaly clay during cyclic suction changes," *Canadian Geotechnical Journal*, vol. 47, no. 6, pp. 688–703, 2010.

[16] H. Sun, D. Mašín, J. Najser, V. Neděla, and E. Navrátilová, "Bentonite microstructure and saturation evolution in wetting–drying cycles evaluated using ESEM, MIP and WRC measurements," *Géotechnique*, vol. 69, no. 8, pp. 713–726, 2018.

[17] R. Thom, R. Sivakumar, V. Sivakumar, E. J. Murray, and P. Mackinnon, "Pore size distribution of unsaturated compacted kaolin: the initial states and final states following saturation," *Géotechnique*, vol. 57, no. 5, pp. 469–474, 2007.

[18] C. Y. Yu, J. K. Chow, and Y.-H. Wang, "Pore-size changes and responses of kaolinite with different structures subject to consolidation and shearing," *Engineering Geology*, vol. 202, pp. 122–131, 2016.

[19] R. de Carteret, O. Buzzi, S. Fityus, and X. F. Liu, "Effect of naturally occurring salts on tensile and shear strength of sealed granular road pavements," *Journal of Materials in Civil Engineering*, vol. 26, no. 6, 2013.

[20] B.-P. Wen and L. He, "Influence of lixiviation by irrigation water on residual shear strength of weathered red mudstone in Northwest China: implication for its role in landslides' reactivation," *Engineering Geology*, vol. 151, pp. 56–63, 2012.

[21] F. Zhang, R. Kong, and J. Peng, "Effects of heating on compositional, structural, and physicochemical properties of loess under laboratory conditions," *Applied Clay Science*, vol. 152, pp. 259–266, 2018.

[22] M. Jiang, F. Zhang, H. Hu, Y. Cui, and J. Peng, "Structural characterization of natural loess and remolded loess under triaxial tests," *Engineering Geology*, vol. 181, pp. 249–260, 2014.

[23] C. W. W. Ng, H. Sadeghi, S. K. B. Hossen, C. F. Chiu, E. E. Alonso, and S. Baghbanrezvan, "Water retention and volumetric characteristics of intact and re-compacted loess," *Canadian Geotechnical Journal*, vol. 53, no. 8, pp. 1258–1269, 2016.

[24] X. Shao, H. Zhang, and Y. Tan, "Collapse behavior and microstructural alteration of remolded loess under graded wetting tests," *Engineering Geology*, vol. 233, pp. 11–22, 2018.

[25] H. Luo, F. Wu, J. Chang, and J. Xu, "Microstructural constraints on geotechnical properties of Malan Loess: a case study from Zhaojiaan landslide in Shaanxi province, China," *Engineering Geology*, vol. 236, pp. 60–69, 2018.

[26] X. Xie, S. Qi, F. Zhao, and D. Wang, "Creep behavior and the microstructural evolution of loess-like soil from Xi'an area, China," *Engineering Geology*, vol. 236, pp. 43–59, 2018.

[27] X.-A. Li, L. Li, Y. Song, B. Hong, L. Wang, and J. Sun, "Characterization of the mechanisms underlying loess

collapsibility for land-creation project in Shaanxi Province, China-a study from a micro perspective," *Engineering Geology*, vol. 249, pp. 77–88, 2019a.

[28] P. Li, W. Xie, R. Y. S. Pak, and S. K. Vanapalli, "Microstructural evolution of loess soils from the Loess Plateau of China," *Catena*, vol. 173, pp. 276–288, 2019b.

[29] J. Xu, Y. Li, C. Ren, S. Wang, S. K. Vanapalli, and G. Chen, "Influence of freeze-thaw cycles on microstructure and hydraulic conductivity of saline intact loess," *Cold Regions Science and Technology*, vol. 181, Article ID 103183, 2021a.

[30] J. Xu, Y. Li, C. Ren, and W. Lan, "Damage of saline intact loess after dry-wet and its interpretation based on SEM and NMR," *Soils and Foundations*, vol. 60, no. 4, pp. 911–928, 2020.

[31] H. J. Gibbs and W. Y. Holland, *Petrographic and Engineering Properties of Loess*, Bureau of Reclamation, US Department of the Interior, Denver, CO, USA, 1960.

[32] J.-D. Wang, P. Li, Y. Ma, S. K. Vanapalli, and X.-G. Wang, "Change in pore-size distribution of collapsible loess due to loading and inundating," *Acta Geotechnica*, vol. 15, no. 5, p. 1081, 2019.

[33] G. R. Gao, "Formation and development of the structure of collapsing loess in China," *Engineering Geology*, vol. 25, no. 2–4, pp. 235–245, 1988.

[34] Y.-H. Wang and W.-K. Siu, "Structure characteristics and mechanical properties of kaolinite soils. I. Surface charges and structural characterizations," *Canadian Geotechnical Journal*, vol. 43, no. 6, pp. 587–600, 2006.

[35] J.-D. Wang, P. Li, Y. Ma, and S. K. Vanapalli, "Evolution of pore-size distribution of intact loess and remolded loess due to consolidation," *Journal of Soils and Sediments*, vol. 19, no. 3, pp. 1226–1238, 2019a.

[36] G. X. Wang, S. F. Xiao, and W. G. Zhou, "Determination of pre-consolidation pressure and structural strength of undisturbed structural soils," *Chinese Journal of Geotechnical Engineering*, vol. 25, no. 2, pp. 249–251, 2003, in Chinese.

[37] L. Chen, J. Li, J. Q. Wang, and Q. Li, "Relationship between structural strength and structural yield pressure of loess," *Chinese Journal of Geotechnical Engineering*, vol. 30, no. 6, pp. 895–899, 2008, in Chinese.

[38] J. Q. Dang and J. Li, "The structural strength and shear strength of unsaturated loess," *Journal of Hydraulic Engineering*, vol. 7, no. 7, pp. 79–83, 2001, in Chinese.

[39] D. Zhang, J. Wang, C. Chen, and S. Wang, "The compression and collapse behaviour of intact loess in suction-monitored triaxial apparatus," *Acta Geotechnica*, vol. 15, no. 2, p. 529, 2019.

[40] E. Romero, G. Della Vecchia, and C. Jommi, "An insight into the water retention properties of compacted clayey soils," *Géotechnique*, vol. 61, no. 4, pp. 313–328, 2011.

[41] Z. Liu, F. Liu, F. Ma et al., "Collapsibility, composition, and microstructure of loess in China," *Canadian Geotechnical Journal*, vol. 53, no. 4, pp. 673–686, 2016b.